AD-A035 503 ROME AIR DEVELOPMENT CENTER GRIFFISS AFB N Y F/G 17/2.1
AN ARRAY TECHNIQUE FOR ZENITH TO HORIZON COVERAGE.(U)
NOV 76 W G MAVROIDES, R J MAILLOUX
UNCLASSIFIED RADC-TR-76-360 NL

1 OF 1
ADA035503



END
DATE FILMED
3-77

ADA035503

RADC-TR-76-360
IN-HOUSE REPORT
NOVEMBER 1976

An Array Technique for Zenith to Horizon Coverage

WILLIAM G. MAVROIDES
ROBERT J. MAILLOUX

Approved for public release: distribution unlimited.

DDC
RECEIVED
FEB 14 1977
D

ROME AIR DEVELOPMENT CENTER
AIR FORCE SYSTEMS COMMAND
GRIFFISS AIR FORCE BASE, NEW YORK 13441

This report has been reviewed by the RADC Information Office (OI) and is releasable to the National Technical Service (NTIS). At NTIS it will be releasable to the general public, including foreign nations.

This technical report has been reviewed and approved for publication.

APPROVED:

PHILIPP BLACKSMITH
Branch Chief, Antenna and Radar Techniques Branch

APPROVED:

ALLAN C. SCHELL
Acting Chief
Electromagnetic Sciences Division

FOR THE COMMANDER:

Plans Office

MISSION
of
Rome Air Development Center

RADC plans and conducts research, exploratory and advanced development programs in command, control, and communications (C^3) activities, and in the C^3 areas of information sciences and intelligence. The principal technical mission areas are communications, electromagnetic guidance and control, surveillance of ground and aerospace objects, intelligence data collection and handling, information system technology, ionospheric propagation, solid state sciences, microwave physics and electronic reliability, maintainability and compatibility.

Printed by
United States Air Force
Hanscom AFB, Mass. 01731

Unclassified

SECURITY CLASSIFICATION OF THIS PAGE (When Data Entered)

REPORT DOCUMENTATION PAGE	READ INSTRUCTIONS BEFORE COMPLETING FORM
1. REPORT NUMBER: RADC-TR-76-360	2. GOVT ACCESSION NO. / 3. RECIPIENT'S CATALOG NUMBER
4. TITLE (and Subtitle): AN ARRAY TECHNIQUE FOR ZENITH TO HORIZON COVERAGE.	5. TYPE OF REPORT & PERIOD COVERED: Inhouse (Technical rept.)
	6. PERFORMING ORG. REPORT NUMBER
7. AUTHOR(s): William G. Mavroides, Robert J. Mailloux	8. CONTRACT OR GRANT NUMBER(s)
9. PERFORMING ORGANIZATION NAME AND ADDRESS: Deputy for Electronic Technology (RADC/ETER), Hanscom AFB, Massachusetts 01731	10. PROGRAM ELEMENT, PROJECT, TASK AREA & WORK UNIT NUMBERS: 62702F, 46001402
11. CONTROLLING OFFICE NAME AND ADDRESS: Deputy for Electronic Technology (RADC/ETER), Hanscom AFB, Massachusetts 01731	12. REPORT DATE: November 1976
	13. NUMBER OF PAGES: 23
14. MONITORING AGENCY NAME & ADDRESS(if different from Controlling Office)	15. SECURITY CLASS. (of this report): Unclassified
	15a. DECLASSIFICATION/DOWNGRADING SCHEDULE

16. DISTRIBUTION STATEMENT (of this Report)

Approved for public release; distribution unlimited.

17. DISTRIBUTION STATEMENT (of the abstract entered in Block 20, if different from Report)

18. SUPPLEMENTARY NOTES

19. KEY WORDS (Continue on reverse side if necessary and identify by block number)

Phased arrays
Wide-angle coverage
Surface wave
Dual mode array

20. ABSTRACT (Continue on reverse side if necessary and identify by block number)

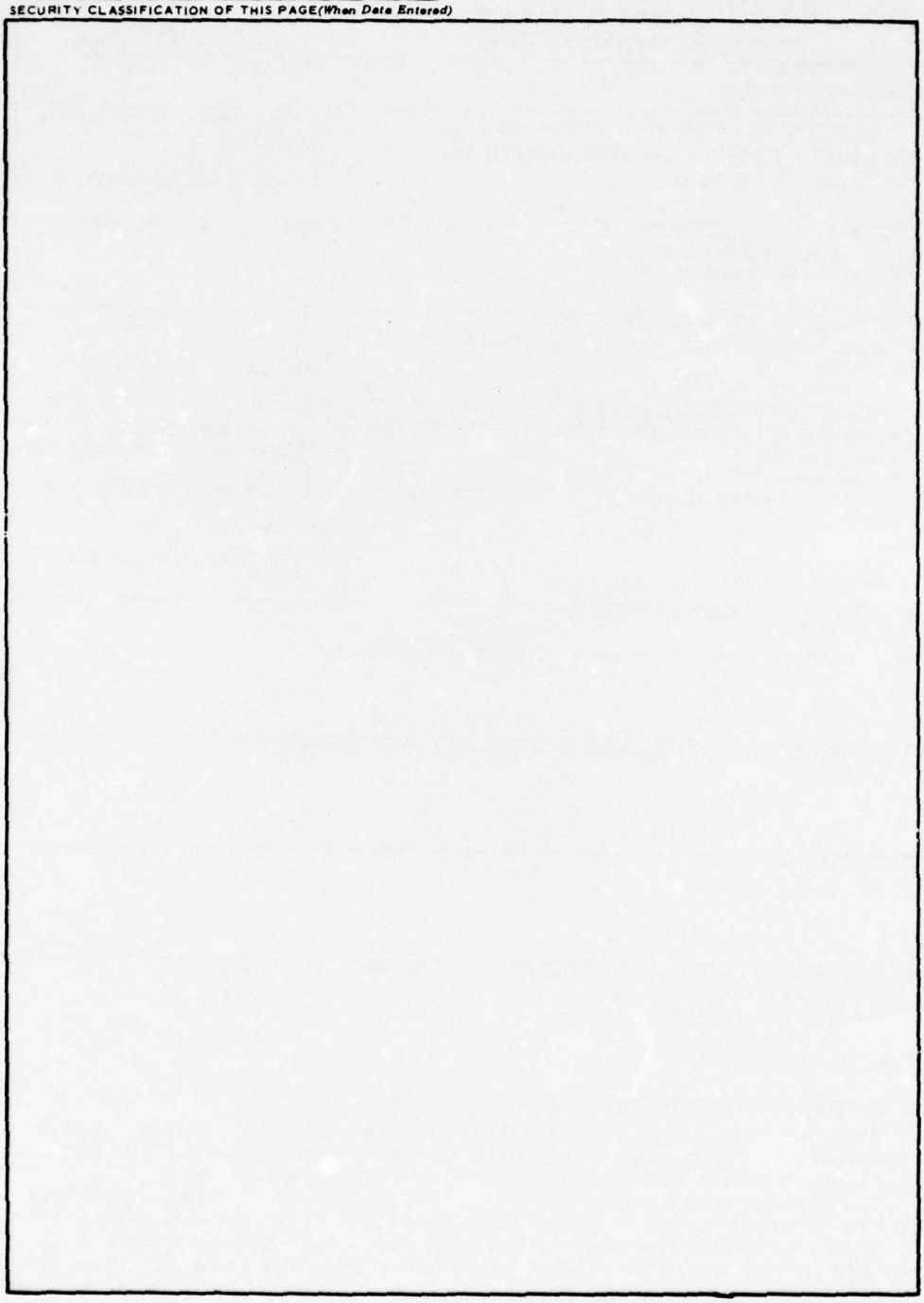
This report describes a new concept in wide-angle coverage arrays and has application to the problem of providing low-cost efficient antennas with hemispherical coverage for aircraft-to-satellite communication links.

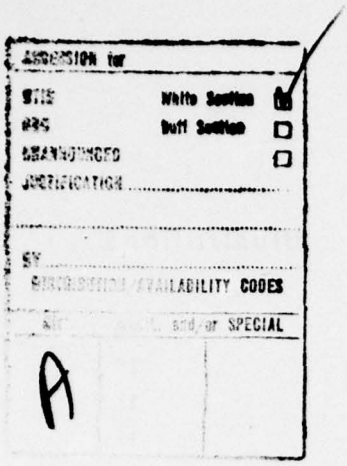
The combined array surface-wave antenna consists of 64 waveguide elements conventionally scanned, except at endfire. At endfire the array is shorted to become a corrugated surface-wave antenna and is excited by an 8-element feed to provide a directional beam near the horizon. The array is rotated to give hemispherical coverage

DD FORM 1 JAN 73 1473 EDITION OF 1 NOV 65 IS OBSOLETE

SECURITY CLASSIFICATION OF THIS PAGE (When Data Entered)

309 050





Contents

1. INTRODUCTION 5

2. PATTERNS FOR THE BASIC ARRAY 7

3. EXPERIMENTAL OPTIMIZATION OF BEAMS NEAR HORIZON 12

4. CONCLUSION 15

REFERENCES 17

APPENDIX A: Design of Feed Elements 19

APPENDIX B: Approximate Formulas for Gain of Flat Arrays Driven to Endfire 21

Illustrations

1. Short-Circuited Array Excited as a Corrugated Surface 7
2. The 64-Element Array and Power Dividers 7
3. The 64-Element Array and 8-Element Column Array Gain at 9.5 GHz 8
4. Array Gain Data 9.0 GHz 9
5. Array Gain Data 9.1 GHz 10
6. Array Gain Data 9.2 GHz 10

DDC
RECEIVED
FEB 14 1977
D

Illustrations

7.	Array Gain Data 9.3 GHz	10
8.	Array Gain Data 9.4 GHz	10
9.	Array Gain Data 9.5 GHz	11
10.	Array Gain Data 9.6 GHz	11
11.	Array Gain Data 9.7 GHz	11
12.	Geometry: Arrays, Feeds and Dielectric Slab	13
13.	Experimental Optimization Patterns: Beam III	14
14.	Comparison of Patterns With and Without Dielectric (Beam IV)	14
15.	Comparison of Patterns With and Without Dielectric (Surface Wave, Beam V)	15
A1.	Details of Coax-to-Waveguide Transition	19

An Array Technique for Zenith to Horizon Coverage

1. INTRODUCTION

Conventionally phased arrays suffer seriously decreased efficiency when scanned to regions near endfire. Typical results for arrays with nominal 20-30 dB gain, mounted on cylinders to simulate an aircraft fuselage, show gain reductions of 7 to 10 dB at endfire compared with broadside radiation, even when the array has been scan matched at angles near endfire.[1,2] Typical aperture efficiencies for such arrays are between 10 and 15 percent at the horizon, because these arrays have 2 to 3 dB additional mismatch loss at broadside. Recent efforts[3,4] have included the use of dielectric structures over or in

(Received for publication 29 November 1976)

1. Borgiotti, G.V. and Balzano, Q. (Sept. 1972) Analysis and element pattern design of periodic arrays of circular apertures on conducting cylinders, IEEE Trans. No. 5 AP-20:547-555.

2. Maune, J.J. (Oct. 1972) An SHF airborne receiving antenna, 22nd Annu. Symp. on USAF Antenna Res. Dev.

3. Balzano, Q., Lewis, L.R., and Swiak, K. (Aug. 1973) Analysis of Dielectric Slab-Covered Waveguide Arrays on Large Cylinders, AFCRL TR 73-0587, Contract F19628-72-C-0202. Scientific Report No. 1.

4. Villeneuve, A.T., Behnke, M.C., and Kummer, W.H. (Dec. 1973) Hemispherically Scanned Arrays, AFCRL TR 74-0084, Contract F19628-72-C-0145, Scientific Report No. 2 (Also see 1974 Int. IEEE Symp. Dig. AP-S:363-366.)

the vicinity of the array, and have shown that these means also improve gain coverage within the hemisphere so that the envelope of peak radiation gain is always within about 6 dB of the maximum radiation over a narrow frequency range. Computations[3] have shown that the coverage obtainable from an array with 23 dB nominal gain presents maximum oscillations of 8 dB over a 10 percent bandwidth and 6 dB over a narrower band. This data was obtained for an array covered with a layer of $\epsilon_r = 4$ material, 0.075λ thick, extending over and beyond the array. These results show encouraging advances over the earlier published work using impedance matching, but, as shown in Appendix B, they still exhibit substantially more gain falloff than would be anticipated if the beamwidth and directivity were those of uniformally illuminated arrays with progressively phased elements[5-8] or optimized surface wave elements.[9,10]

A new concept in wide-angle coverage arrays is investigated in this experimental program and has application to the problem of providing low cost, efficient antennas with hemispherical coverage for aircraft-to-satellite communication links. This concept involves the use of a dual mode radiating structure consisting of a conventional waveguide phased array and the added feature that each waveguide can be short-circuited to form a corrugated surface for endfire radiation. The phased array is, therefore, used over a wide angle scanning range, but is not required to provide radiation at endfire. Endfire radiation is obtained by exciting the shorted corrugated structure with a separate waveguide feed. The array is rotated to give hemispherical coverage.

This report describes the results of an experimental program designed to test the validity of this concept. Quoted values of gain were measured by comparison with a standard gain horn. Data were repeatable to within ±.5 dB.

---

5. Walter, C.H. (1965) Traveling Wave Antennas, McGraw Hill Book Co., New York, pp. 121-122, 322-325.

6. Zakharyev, I., Lemanski, A., and Shcheglov, K. (1970) Radiation from apertures in convex bodies (flush-mounted antennas), The Golden Press, Boulder, Colorado, Chap. 2.

7. Bickmore, R.W. (Apr. 1958) A note on the effective aperture of electrically scanned arrays, IRE Trans. **AP-6**:194-196.

8. Elliott, R.S. (Jan. 1964) Beamwidth and directivity of large scanning arrays; last of two parts, Microwave Journal, pp. 74-82.

9. Hansen, W.W. and Woodyard, J.R. (March 1938) "A New Principle in Antenna Design," Proc. IRE, **26(3)**:333-345.

10. Ehrenspeck, H. and Poehler, H. (Oct. 1959) A new method for obtaining maximum gain from yogi antennas, IRE Trans. **AP-7**:379-385.

2. PATTERNS FOR THE BASIC ARRAY

Figure 1 shows an array of 64 waveguide elements excited as a corrugated structure by an eight-element surface-wave feed. The array is also excited by a 64-way power divider and eight phase shifters to form a beam scanned in the elevation plane, as shown in Figure 2. In practice, the waveguides would be short-circuited by diodes or mechanical shutter switches to form the corrugated

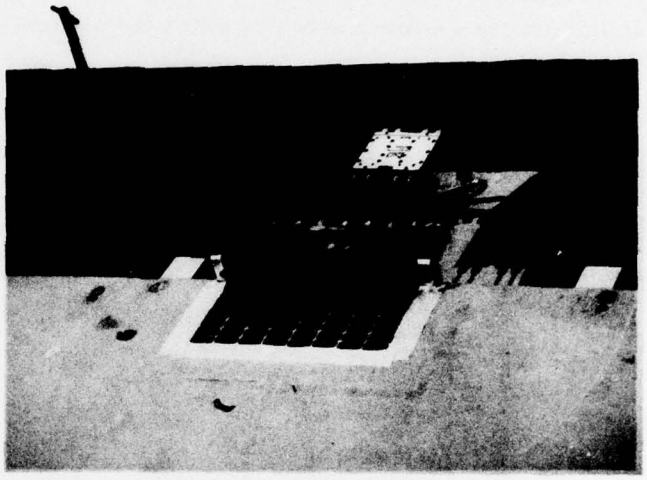


Figure 1. Short-Circuited Array *Excited as a* Corrugated Surface

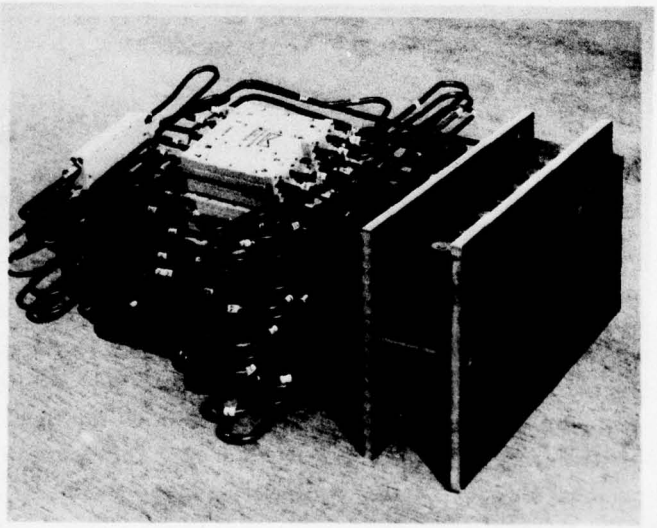


Figure 2. The 64-Element Array and Power Dividers

surface for endfire radiation, but the experiment was conducted using fixed short circuits placed 1 in. from the radiating end of each waveguide. This distance corresponds to slightly more than $3\lambda g/4$, so the corrugated surface has a capacitive surface.

The waveguides are standard x-band guides, with 0.050-in. walls, having outer dimensions of .5 in. x 1.0 in. The 8 x 8 array thus measures 8 in. x 4 in. The ground plane, partially shown in Figure 1, measured 6-ft wide and had a 4-ft curved surface with an 84 in. radius extending in front of the antenna structure.

Figure 3 shows the envelope of beam peaks indicating measured array gain at 9.5 GHz for a number of beams within the sector. Included is one beam

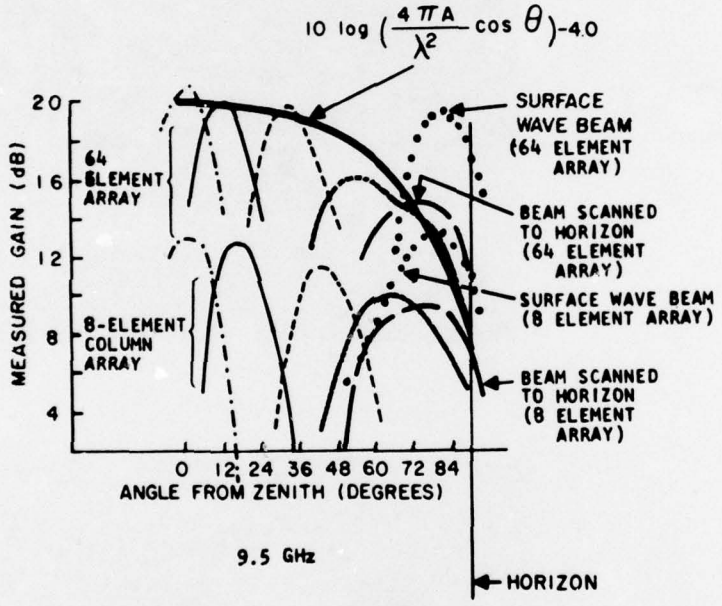


Figure 3. The 64-Element Array and 8-Element Column Array Gain at 9.5 GHz

scanned to the horizon and one formed by the excited corrugated structure. The various beam peaks are distinguished by using differently coded lines in the figures. Within each column the elements were excited with progressive phase angles $n\phi$, where ϕ takes on the values of 0° for Beam 0, 45° for Beam I, 90° for Beam II, 135° for Beam III, and 145° for Beam IV. The endfire beam generated by the surface wave structure is Beam V. At the designated center

frequency 9.5 GHz, the computed beam radiation angles for beams zero through four are 0°, 18°, 38°, 69°, and endfire. The actual beam angles as shown in the figures differ from these angles because of the cumulative effect of mutual coupling and element pattern falloff. The data show that the surface wave beam provides approximately 6 dB gain increase at the horizon as compared with the scanned endfire beam, and that, in fact, the achievable gain at the horizon is 17 dB; this is only 4 dB below the maximum, and the peak at 80° is nearly equal to the broadside gain. The minimum of the pattern gain envelope occurs at about 69°, and shows a dip to approximately 16 dB. The figure also shows the available area gain projected to the various spatial angles. At 9.5 GHz the measured broadside gain is 21 dB and the peak gain for the endfire beam is 19.6 dB (at 80°). Measurements of power divider and beam former circuit loss have revealed that the total loss through the 64-element power divider and waveguide to coaxial line transitions is approximately 4 dB, and when the endfire circuit is used the measured total feed loss is approximately 1.8 dB. Measured directivities are, therefore, approximately 25 dB at broadside and 21.4 at 80°.

Measured beamwidths have been correlated with these gain measurements. The observed H-plane beamwidth at 9.5 GHz is 8° for all scan angles and the E-plane beamwidth is 16° for the broadside beam and 19.8° for the surface wave endfire beam. If the assumption is made that these beam structures have ideal sector coverage out to the 3 dB points, with directivity given by 4π divided by the beamwidths (radians) in each plane, then these measured beamwidths are consistent with directivities of 25 at broadside, and 24.2 at 80°. The measured directivity at 80° is lower because the beam formed by the surface wave is far from a pencil beam and has substantial radiation at angles well above the horizon. Figures 4 through 11 show this effect.

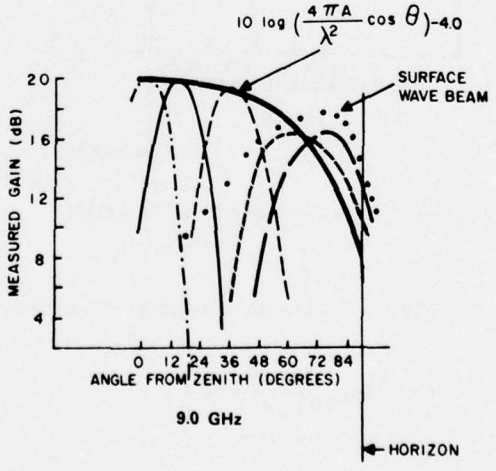


Figure 4. Array Gain Data 9.0 GHz

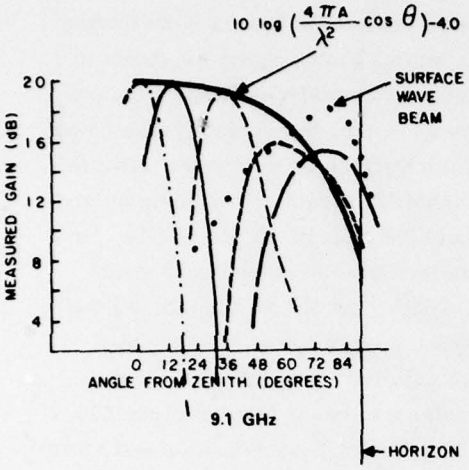


Figure 5. Array Gain Data 9.1 GHz

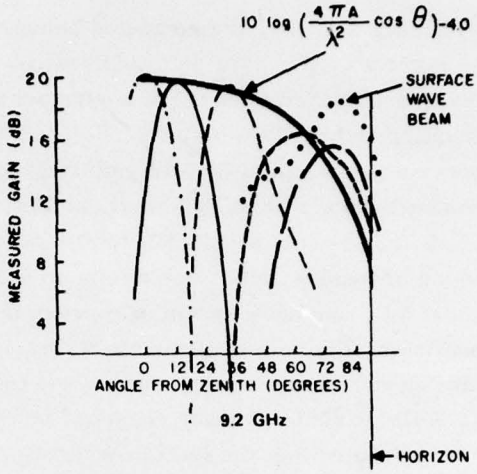


Figure 6. Array Gain Data 9.2 GHz

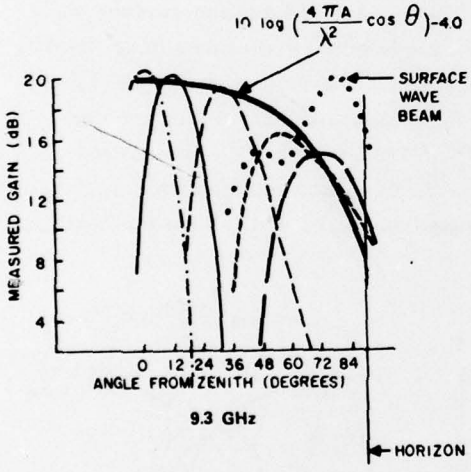


Figure 7. Array Gain Data 9.3 GHz

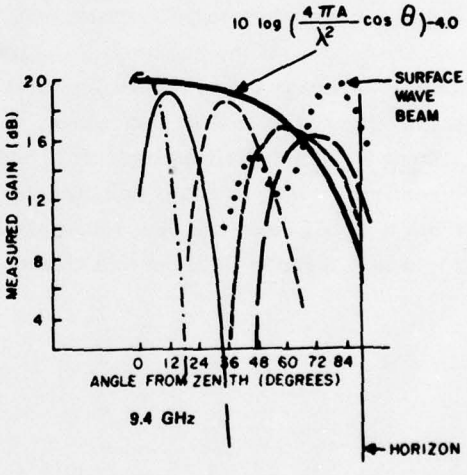


Figure 8. Array Gain Data 9.4 GHz

Figure 3 also shows the locus of the curve:

$$f = 10 \log_{10}\left(\frac{4\pi A}{\lambda^2} \cos \theta\right) - 4.0.$$

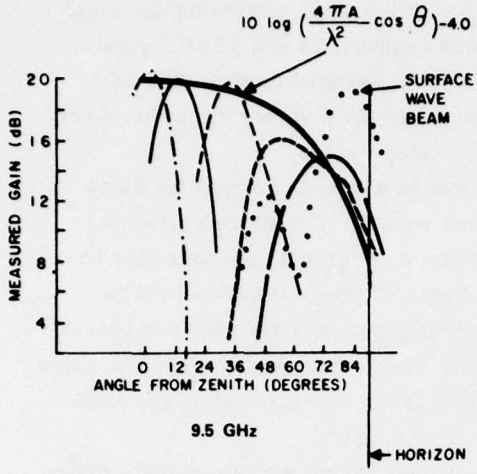


Figure 9. Array Gain Data 9.5 GHz

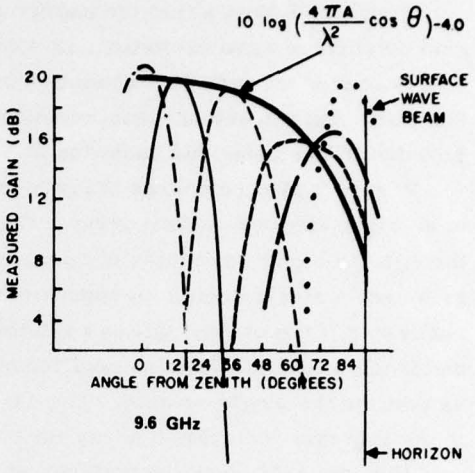
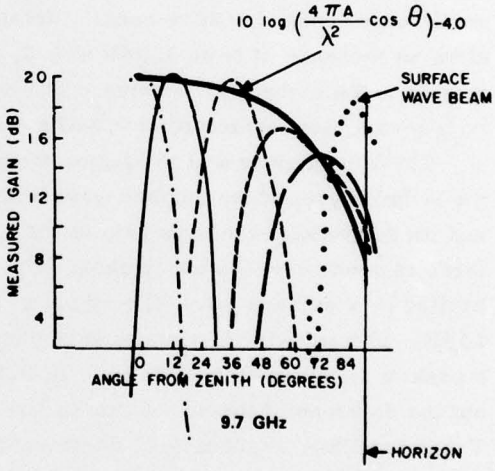


Figure 10. Array Gain Data 9.6 GHz

Figure 11. Array Gain Data 9.7 GHz



This is the calculated area gain reduced by the measured feed circuit loss, and should be a good approximation to the projected gain except near endfire. The gain, whether measured directly or calculated from measured beamwidth, is approximately one dB above this value at broadside; a result due apparently to edge effects in the small array.

Appendix B shows that the endfire gain for this array, assuming optimum gain or surface wave excitation, is somewhere between 24 and 23 dB. Again, this is consistent with the calculation based upon measured beamwidths at 80° (24.2 dB), but the actual measured directivity of 21.4 dB shows a loss of nearly 3 dB due to the undesired radiation at higher angles.

Figure 3 also compares the patterns of the 64-element array with those of an eight-element column array. Consistent with the 1.8 dB measured loss through the eight-way power divider, for beams 0, I, and II, the increase in gain over a single column is approximately 7 dB. A nine-dB gain would be realizable if the cables, fittings and the eight-way power dividers were lossless, and if the average reflection coefficient for the 64-element array were the same as that for the single column. The 64-element array has approximately 6 dB more gain than the column array for beams III through V.

Figures 4-11 show the patterns of the scanned beams and the surface-wave beam of the combined array-surface wave antenna at frequencies 9-9.7 GHz at 0.1 GHz intervals. In all cases there is an increase in gain for Beam V (surface wave beam) over Beam IV, and at most frequencies the peak of the surface wave formed beam is several degrees closer to the horizon than Beam IV, the conventionally scanned endfire beam. Relative gain measurements at the horizon show an increase of from 3.5 dB at 9.0, 9.1 and 9.2 GHz to 5.5 and 6 dB increase in gain at the higher frequencies. The curves also show the area gain (directivity minus loss) evaluated at 9.5 GHz for the purposes of comparison.

These data show that the major factors that establish bandwidth limits are the reduced gain of the surface wave beam at the low end of the frequency band and its somewhat excessive gain at the high end. Figure 4 shows that at 9.0 GHz there is good coverage out to about 84°, but the beam of the corrugated structure excited by a surface wave is very broad and so the horizon gain falls to about 15 dB. The gain of the surface wave beam increases with frequency, reaching a peak at approximately 9.6 GHz. At 9.7 GHz the horizon gain is still very high, but the envelope of the set of curves has a dip to the 15 dB level at about 75°. Taken together, Figures 4-11 document that the technique can be used to design an antenna with nominal gain 21 dB at 9.5 GHz and with zenith-to-horizon gain contours exceeding 16 dB over the 5 percent bandwidth from 9.1 to 9.6 GHz. The system gain exceeds 15 dB over the entire 7.5 percent band.

3. EXPERIMENTAL OPTIMIZATION OF BEAMS NEAR HORIZON

Several experiments were conducted in an attempt to optimize the gain and angle of scan of the array at the lower angles, that is, Beams III, IV and V.

The first experiment consisted of placing a sheet of thin metal over the openings of the waveguide feeds of the surface-wave exciter. Throughout Figures 3-11 these waveguides had been terminated in a matched load, but in this particular experiment the surface of covered waveguides constituted a reflecting fence 0.5 in. high, located at the back edge of the 64-element array. The second experiment consisted of placing a thin sheet of plexiglass dielectric directly in front of and abutting the 64-element array. The sheet dimensions were 0.060-in. thick, 8-in. wide, and 5-in. long.

Figure 12 shows a sketch of these modifications to the array and Figure 13 shows the basic array patterns (solid) for beam III, compared with those taken using the dielectric sheet (dashed), with the surface wave exciters covered (dash-dotted), and with both the sheet and covered exciters (dotted). In general, the use of shorted exciter waveguides alone raised the gain for beam III (and, although not shown, that of beam IV) by 0.5 to 1.0 dB. Using a dielectric slab alone (dashed) also increased the peak gain for this beam, but produced a minimum near 69°. This minimum became deeper when both modifications were used together (dotted).

Figures 14 and 15 compare the basic array patterns (solid) with those for the array with dielectric (dashed) for beam IV and the surface wave beam V. Figure 15 shows that adding the dielectric slab increased the gain of these two beams and caused the surface wave beam to bend more toward the horizon to produce a further gain increase at that point. Unfortunately, the minimum

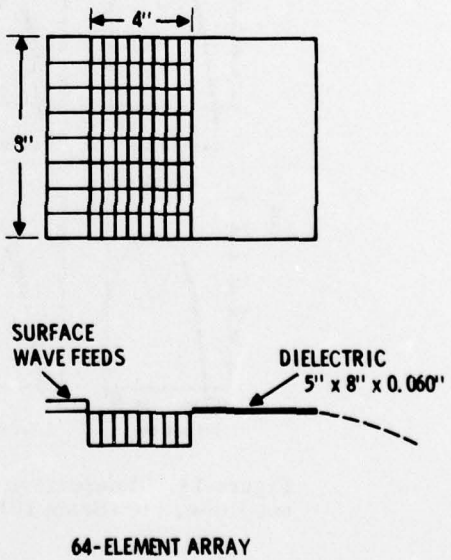


Figure 12. Geometry: Arrays, Feeds and Dielectric Slab

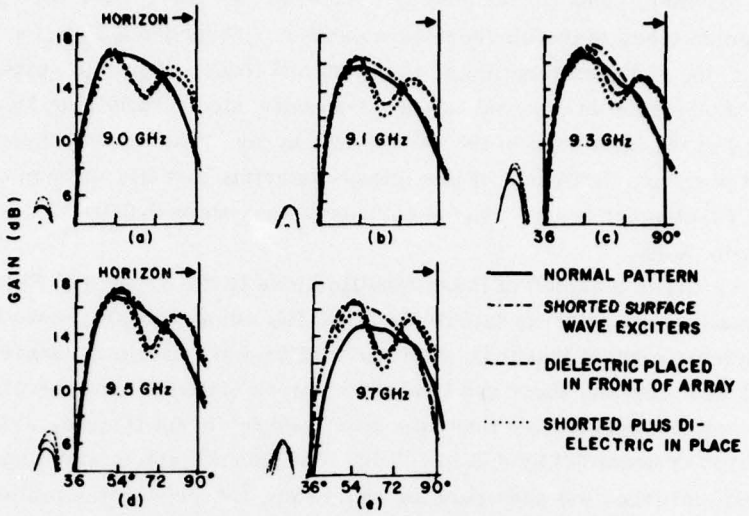


Figure 13. Experimental Optimization Patterns: Beam III

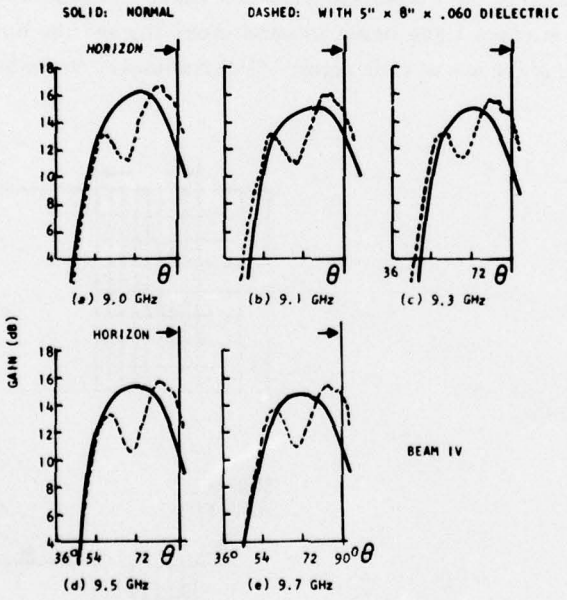


Figure 14. Comparison of Patterns With and Without Dielectric (Beam IV)

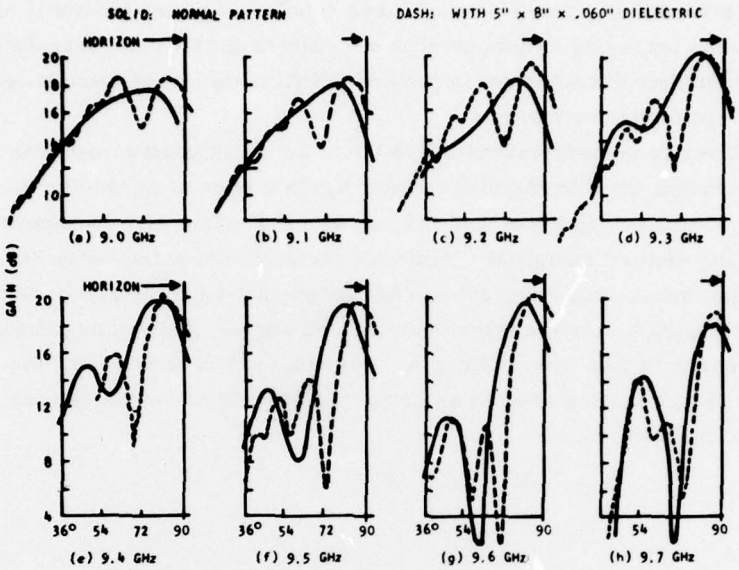


Figure 15. Comparison of Patterns With and Without Dielectric (Surface Wave, Beam V)

observed at 69° for beam III remained at approximately the same angle for beams IV and V, and thus there is no beam that produces adequate coverage near 70° for the array with dielectric slab. The demonstration of increased coverage at the horizon does, however, support the results obtained by Balzano et. al.[3] who have performed a numerical optimization of a similar dielectric loaded geometry, and have found that such loading can produce strong radiation at the horizon, but that this is nearly always accompanied by a region of minimum gain at some higher elevation angle.

4. CONCLUSION

These experiments were undertaken in an attempt to exploit the potential of using the short-circuited surface of a conventional array to form an efficient beam near the horizon. The array is phased according to normal practice to scan a beam throughout a wide sector of space, but the array is shorted at the horizon and its front surface is excited by a surface-wave launcher.

Results indicate that the technique can provide gain within 5 dB of the broadside gain over approximately a 5 percent bandwidth, and within 6 dB of

broadside over a 7.5 percent band. These results compare favorably with other techniques for achieving hemispherical scan and it is felt that these data establish a basis for further development in the area of flush-mounted antenna techniques with zenith-to-horizon coverage.

In addition to measurements of the basic array structure, several other sets of measurements were performed to investigate means of enhancing the horizon coverage. Chief among these was the use of a dielectric slab to support a surface wave for endfire radiation. Although certainly not exhaustive, this data revealed that substantial horizon gain enhancement can be obtained, but not without sacrificing gain at some intermediate scan angle. Recommendations for future research in this area include a theoretical effort to optimize the scanning characteristics of such an array and a study of techniques for mechanical implementation.

References

1. Borgiotti, G.V. and Balzano, Q. (Sept. 1972) Analysis and element pattern design of periodic arrays of circular apertures on conducting cylinders, IEEE Trans. No. 5 **AP-20**:547-555.

2. Maune, J.J. (Oct. 1972) An SHF airborne receiving antenna, 22nd Annu. *Symp. on USAF Antenna Res. Dev.*

3. Balzano, Q., Lewis, L.R., and Swiak, K. (Aug. 1973) Analysis of Dielectric Slab-Covered Waveguide Arrays on Large Cylinders, AFCRL TR 73-0587, Contract F19628-72-C-0202. Scientific Report No. 1.

4. Villeneuve, A.T., Behnke, M.C., and Kummer, W.H. (Dec. 1973) Hemispherically Scanned Arrays, AFCRL TR 74-0084, Contract F19628-72-C-0145, Scientific Report No. 2. (Also see 1974 Int. IEEE Symp. Dig. **AP-S**:363-366.)

5. Walter, C.H. (1965) Traveling Wave Antennas, McGraw Hill Book Co., New York, pp. 121-122, 322-325.

6. Zakharyev, I., Lemanski, A., and Shcheglov, K. (1970) Radiation from apertures in convex bodies (flush-mounted antennas), The Golden Press, Boulder, Colorado, Chap. 2.

7. Bickmore, R.W. (Apr. 1958) A note on the effective aperture of electrically scanned arrays, IRE Trans. **AP-6**:194-196.

8. Elliott, R.S. (Jan. 1964) Beamwidth and directivity of large scanning arrays; last of two parts, Microwave Journal, pp. 74-82.

9. Hansen, W.W. and Woodyard, J.R. (March 1938) "A New Principle in Antenna Design," Proc. IRE, **26(3)**:333-345.

10. Ehrenspeck, H. and Poehler, H. (Oct. 1959) A new method for obtaining maximum gain from yogi antennas, IRE Trans. **AP-7**:379-385.

Appendix A

Design of Feed Elements

An array of this type with the 64 elements adjacent to each other necessitated end-on transitions with the coax and waveguide being colinear; the frequency range was chosen between 9.0 and 10.0 GHz with VSWR $\leq$ 1.5.

OSM-size fittings were used to accommodate the x-band guide. Flange-mounted connectors were used for ease in mounting and modified by soldering copper tubing (1/8 in. diam) over the existing center conductor. The tubing was flattened and bent over to one of the broad faces of the waveguide to form a coupling loop. A tuning screw 1/8 in. from the loop (see Figure A1) provided adequate adjustment for impedance matching to the 50 ohm coaxial line.

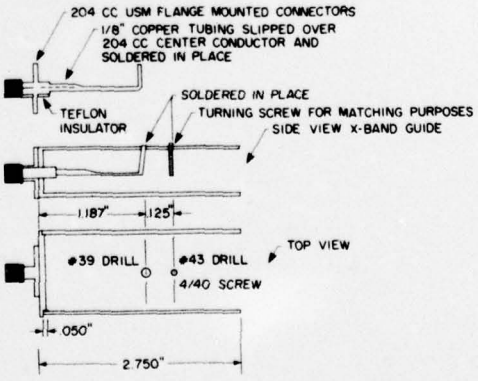


Figure A1. Details of Coax-to-Waveguide Transition

PRECEDING PAGE BLANK-NOT FILMED

Appendix B

Approximate Formulas for Gain of Flat Arrays Driven to Endfire

A number of authors give simple relations for the endfire and optimum gain for Yagi's and other endfire structures. This Appendix compares these and gives some approximate results for flat arrays driven to endfire. In addition to serving as a catalog for these basic and simple engineering references, the purpose of the Appendix is to give some approximate bounds for maximum gain at endfire for a flat array mounted on a groundplane.

The directivity of a uniform column of isotropic elements is given by

$$D \sim C\, L/\lambda \tag{B1}$$

where L is the length of the line source and C is a constant. The value of C is approximately 2 for broadside, 4 for a large array at endfire or for a large array with optimum endfire gain (since the Hansen-Woodyard or Ehrenspeck-Poehler results give $c/v \sim 1$ for a large array). For short sources ($3\lambda \leq L \leq 8\lambda$) the value of C is approximately 7 for uniformally illuminated arrays with optimized[5] phase constant $\beta > ko$, and can reach the value of 10 when the optimization is carried out to include the source radiation (and hence for a non-uniform illumination).

PRECEDING PAGE BLANK-NOT FILMED

Assuming that the endfire or optimum endfire pattern is approximately a pencil beam, the beamwidth is:

$$\theta \doteq \sqrt{\frac{4\pi}{D}} \doteq \sqrt{\frac{4\pi}{C}\ \frac{\lambda}{L}} \tag{B2}$$

Now consider a flat array with dimensions L_1 in the plane of scan, and L, in the plane perpendicular to scan. For uniform illumination in the plane of L_2, the beamwidth in that plane is approximately $\theta_2 = \lambda / L_2$ and so the approximate gain for the flat array for the various endfire conditions is:

$$D \doteq \frac{4\pi}{\theta_1 \theta_2} \doteq \sqrt{4\pi C}\left(\frac{L_2}{\lambda}\right)\sqrt{L_1/\lambda} \tag{B3}$$

This result is consistent with those obtained exactly at endfire by Bickmore[7] and by Elliott[8] if the factor C = 3.546 is used.

Eq. 3 predicts that for arrays that are short in the scan plane one might achieve a gain improvement of $\sqrt{10/3.55}$ or approximately 2.2 dB, by using an optimized gain design for which the constant C is 10. Although the value of 10 can be obtained for short surface-wave line sources, or arrays with unequal amplitude distributions, as obtained by optimizing the combined radiation of the source and the surface-wave structure, this number is higher than what can be attained with equal element excitation and progressive phase. Figure 3-27 of reference five shows a curve of parameter C for various lengths of column arrays in that case and indicates that more typical values range between 7 and 8 for L_1 between 3 and 10 wavelengths.

The equations for directivity given above assume that the array consists of free space isotropic elements and hence there is no element factor implied that would further constrain the pattern. Assuming that the structure is mounted on a flat or a large curved ground plane, the directivity will be increased by approximately 3 dB over that given in Eq. 3.

At endfire, the ratio of this directivity to the broadside directivity $4\pi L_1 L_2 / \lambda^2$ (which also assumes half-space element patterns) is given below:

$$\frac{D}{D_o} = \sqrt{\frac{C}{\pi}}\sqrt{\frac{\lambda}{L_1}} \tag{B4}$$

The most obvious conclusion that one can base upon this equation is that for any given gain it is advantageous to decrease L_1 as much as possible, for this minimizes the scan loss.

Several examples are given below to show the relative gain at the horizon for a 20 dB square array ($L/\lambda \sim 2.8$), a 30 dB square array ($L/\lambda \sim 8.9$), and the array structure studied in this report ($L/\lambda = 3.22$ at 9.5 GHz).

Example 1: 20 dB square array

$10 \log \frac{D}{D_o}$ = -0.5 dB for C = 7 optimum gain array (uniform progressive phase)

= -2.0 for C = 3.55 endfire array

Example 2: 30dB square array

$10 \log \frac{D}{D_o}$ = -3 dB for C = 7 optimum gain array

= -4.5 for C = 3.55 endfire array

Example 3: 3.22λ array at 9.5 GHz

$10 \log \frac{D}{D_o}$ = -0.0 for C = 10 array excited as optimum corrugated surface

= -0.77 for C = 7 optimum gain array

= -2.25 for C = 3.55 endfire array